IIETA International Information and Engineering Technology Association
Advancing the World of Information and Engineering

Traitement du Signal
Vol. 41, No. 5, October, 2024, pp. 2655-2661
Journal homepage: http://iieta.org/journals/ts

Discrete Cosine Transform-Based Kernel Discriminant Analysis for Enhanced Biometric Recognition

Wenying Ma

Zibo Vocational Institute, Zibo 255300, China

Corresponding Author Email: 10799@zbvc.edu.cn

https://doi.org/10.18280/ts.410538

Received: 7 May 2024
Revised: 12 September 2024
Accepted: 8 October 2024
Available online: 31 October 2024

Keywords:
biometrics, DCT, KDA, feature extraction, face recognition, FERET database, AR database

ABSTRACT

This study presents a comprehensive exploration of the Discrete Cosine Transform (DCT) and its application in biometric recognition systems, with a specific focus on improving the discriminative capabilities of existing methods. The inherent properties of the DCT are leveraged, and the traditional Linear Discriminant Analysis (LDA) framework is extended to nonlinear scenarios through the design of a novel DCT-based Kernel Discriminant Analysis (DCT-KDA) algorithm. The proposed approach integrates the advantages of DCT with the flexibility of kernel methods to achieve enhanced feature extraction and classification performance. Rigorous experiments are conducted using the FERET and AR face databases to evaluate the effectiveness of the algorithm under various conditions. Results demonstrate that the DCT-KDA method consistently outperforms conventional techniques such as standard KDA and DCT-LDA, delivering superior recognition accuracy and faster computational performance. These improvements highlight the potential of the proposed DCT-KDA framework for real-time biometric applications. By providing a robust, efficient, and scalable solution, this research contributes to advancing the field of biometric recognition, offering insights into both theoretical developments and practical implementations.

1. INTRODUCTION

Biometric identification is essentially the feature recognition of images, and for image recognition, extracting effective image features is the first task to complete the recognition. Image features are used to distinguish the most basic attributes or characteristics within an image, they can be natural features that can be identified by human vision in the original image; or they can be obtained by measuring and processing the image to obtain certain features or parameters, and finally they become artificial features.

The use of biometric identification can be traced back to ancient Egypt, where individuals were identified by measuring the dimensions of various parts of the human body. Among the earliest and most enduring biometric modalities are facial recognition and fingerprint identification. Numerous studies on facial recognition have been conducted both domestically and internationally, employing a variety of approaches and techniques. Statistical feature-based recognition methods represent faces as algebraic feature vectors, and the most representative ones are Principal Component Analysis (PCA) and LDA [1-3]. On the basis of PCA, Arisandi et al. [4] proposed the Fisherface method based on the Fisher criterion. Kernel-based nonlinear feature extraction technique is also a rapidly developing new direction in the current pattern recognition field, which was initially proposed by Zhou Bo and applied in Support Vector Machine (SVM) [5, 6]. Mika et al. proposed to implement nonlinear discriminative analysis, i.e., Kernel Fisher Discriminative Analysis (KFDA) using kernel functions [7]. Zhao and Yuen [8] explored the relationship between the human face and its spectral characteristics, revealing that changes in facial expression and minor occlusions primarily affect local light intensity flow, known as the Intensity Manifold Phenomenon. As a result, one of the emerging research directions involves using time-frequency domain tools to filter out high-frequency information, with low-frequency images being employed to represent key biometric features. Lee and Krim [9] discovered that the degree of energy aggregation in the frequency domain correlates with the sparseness and depth of texture in palmprint images within the spatial domain. Antonijevic et al. [10] applied the fractional Fourier transform to face recognition. Hasimah et al. [11] proposed the Fourier-LDA (F-LDA) and applied it to face recognition and achieved good classification results.

The frequency-domain-based biological feature extraction method involves transforming the original spatial-domain biological image into the frequency domain. Various frequency-domain features, such as amplitude and phase information, are then employed to classify the image, a process commonly referred to as spectral analysis. The DCT is a widely used spectral analysis technique. It converts face images into the frequency domain, allowing the extraction of DCT coefficients, which serve as features for recognition. In this approach, face recognition with DCT focuses on extracting the low-frequency coefficients from the DCT frequency domain of an initial image set to build a feature library [12]. The same method is applied to extract the low-frequency coefficients from the image to be recognized. The simplified information (coefficients) from the target image is then compared against the stored coefficients in the feature library to determine the recognition outcome [13].

The advantages of using the DCT for face recognition stem from several of its outstanding properties [14-16]: (1) DCT coefficients provide an excellent description of image features, offering a strong advantage in capturing and representing image information; (2) while the Karhunen–Loève Transform (KLT) achieves optimal energy compression, the energy concentration efficiency of DCT is nearly equivalent. Additionally, DCT relies on data-independent fixed bases and benefits from fast algorithms, making DCT-based recognition systems simple and computationally efficient; (3) the features of two-dimensional images transformed by DCT are inherently scale-invariant; and (4) since the JPEG compression standard, widely used for face image storage, employs DCT, it is essential to develop and refine face recognition techniques within the DCT domain.

In the field of face recognition, the DCT is primarily employed for feature extraction, with various approaches utilizing DCT features for classification. Beyond face recognition, DCT has also been applied in related areas. Benziane et al. [17] introduced a novel color video watermarking technique based on the one-dimensional DCT. Gomez-Coronel et al. [18] proposed a robust and secure watermarking approach using a combination of the Hermite Transform (HT) and the Singular Value Decomposition-DCT (SVD-DCT), leveraging the HT and DCT to provide a spatial-frequency representation of grayscale images. Additionally, Zhang and Zhou [19] developed a new method called Structured Orthogonal Random Features based on DCT (SORF-DCT) to approximate Gaussian kernel functions, offering a computationally efficient alternative in kernel-based machine learning applications.

This paper examines a classical frequency-domain discriminative analysis technique and its application in biometric recognition. To enhance the traditional DCT-based discriminative analysis approach, a nonlinear discriminative analysis algorithm leveraging the DCT is proposed and applied to face recognition. The method begins by applying the DCT to face images and selecting suitable frequency bands. The KDA method is then employed to extract nonlinear discriminative features from these bands. The proposed algorithm not only enhances recognition accuracy but also achieves faster recognition speeds.

The remainder of the paper is structured as follows: the next section presents a detailed description of the proposed methodology, followed by the experimental setup and analysis of results. The final section provides the conclusions.

2. DCT CONVERSION AND FREQUENCY BAND SELECTION

2.1 DCT

The DCT is an excellent data compression method and its data compression capability is second only to the KLT. For a digital image $X(x,y)$ of size $M \times N$, its 2D DCT is defined as:

$$Y(u,v)=a(u)a(v) \sum_{x=0}^{M-1}\sum_{y=0}^{N-1} X(x,y)\cos[\frac{(2x+1)u\pi}{2M}]\cos[\frac{(2y+1)v\pi}{2N}] \tag{1}$$

where, $u=0,1,2,\cdots,M-1$, $v=0,1,2,\cdots,N-1$; $Y(u,v)$ are the DCT coefficients; $a(u)$ and $a(v)$ are defined as follows:

$$a(u)=\begin{cases}\sqrt{1/M}, u=0\\ \sqrt{2/M}, u=1,2,\cdots,M-1\end{cases} \tag{2}$$

$$a(v)=\begin{cases}\sqrt{1/N}, v=0\\ \sqrt{2/N}, v=1,2,\cdots,N-1\end{cases} \tag{3}$$

The DCT inverse transform equation is:

$$X(x,y)=\sum_{u=0}^{M-1}\sum_{v=0}^{N-1} Y(u,v)a(u)a(v) \cos[\frac{(2x+1)u\pi}{2M}]\cos[\frac{(2y+1)v\pi}{2N}] \tag{4}$$

where, $x=0,1,2,\cdots,M-1$, $y=0,1,2,\cdots,N-1$.

The 2D DCT converts an image into a coefficient matrix of the same size as the original image. This matrix contains both low- and high-frequency components. The low-frequency components, which represent the slowly varying parts of the image and carry its primary information, are concentrated in the upper-left corner of the matrix. In contrast, the high-frequency components, located in the lower-right corner, capture fine details and edges, but they primarily contain noise and other less relevant information. During the reconstruction process using the inverse DCT, only a small subset of the low-frequency components needs to be retained, while most of the high-frequency components can be discarded. This selective retention allows for the recovery of an image that closely resembles the original, with minimal perceptible loss.

DCT has the following properties for image compression and feature representation:

(1) In terms of energy compression, DCT is second only to the KLT as an image compression method and uses a data-independent fixed basis;

(2) DCT is an orthogonal transformation that reduces the correlation of random vectors to some extent;

(3) DCT low frequency coefficients describe the image features well and can be used for frequency domain feature extraction;

(4) The features of a 2D image transformed by DCT are scale invariant;

(5) DCT has rapid implementation algorithms.

2.2 DCT band selection method

Given a sample set of greyscale images X, where each of the greyscale images $f(x,y)$ is of size $C \times D$ and $1 \leq x \leq C$, $1 \leq y \leq D$, $C \geq D$. A 2D DCT is done on each image, and Figure 1 shows the original image (a) as well as the transformed image (b). From (b), it can be seen that most of the energy information of the image is concentrated in the upper left corner of the image, i.e., the low frequency part.

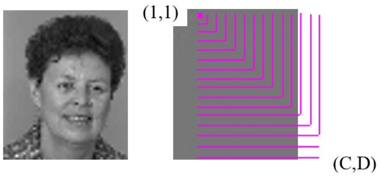

(a) (b)

Figure 1. Schematic diagram of DCT transformation

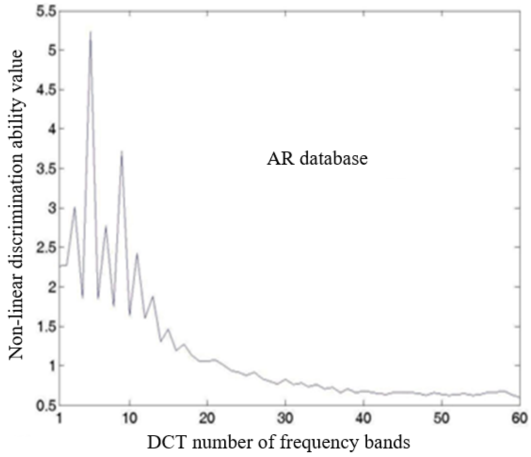

(a) AR database

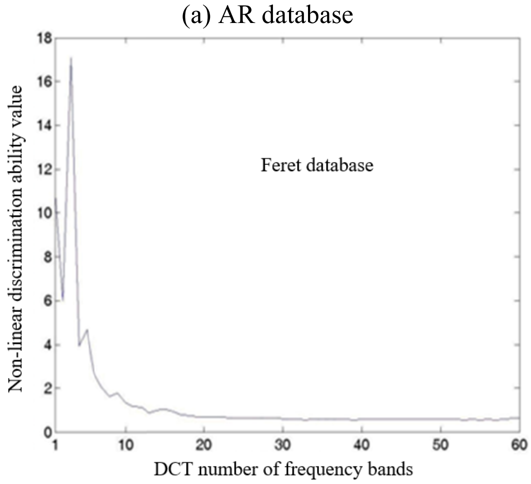

(b) FERET database

Figure 2. Nonlinear discrimination capability values for all DCT bands

We use the half-square ring $Ring(k)$ to represent the first k bands:

$$F(u,v) \in Ring(k),\ 1 \le k \le C \tag{5}$$

If the k-th band is selected, then the values corresponding to that band in the transformed image are retained; otherwise, these values are set to zero.

Nonlinear discriminative analysis methods usually use kernel function-based methods to achieve nonlinear mapping from low-dimensional space to high-dimensional space. In this paper, the following method will be used to compute the nonlinear discriminative ability of the k-th DCT band in the DCT transformed image.

As shown in Figure 1, if the k-th DCT band is selected, then the corresponding $F(u,v)$ value is retained using Eq. (10). The k-th DCT band of each image in the sample set is converted into the form of a vector, and the corresponding inter-class scatter matrix $S_B^{'\phi}$ and intra-class scatter matrix $S_W^{'\phi}$ are constructed.

Then, the nonlinear discriminative power of the k-th band in the DCT transformed image F_k can be calculated by using the Fisher criterion in the feature space:

$$F_k = \frac{tr(S_B^{'\phi})}{tr(S_W^{'\phi})} \tag{6}$$

where, $tr(\ )$ denotes the trace of the matrix.

Figure 2 illustrates the nonlinear discriminative capabilities of DCT bands on the AR and FERET face databases. For the experiments, three images per individual were used as training samples. The data from Figure 2 shows that lower DCT bands generally offer higher discriminatory power. Consequently, a number of low-frequency bands can be selected sequentially to achieve the best recognition results.

3. NONLINEAR DCT DISCRIMINATIVE FEATURE EXTRACTION

As described in the previous section, all the face images in the sample set X are DCT transformed, and a number of low-frequency bands are selected and vector quantized for each image according to the nonlinear discriminative ability to form a new sample set $X' = \{z_1, z_2, \cdots, z_N\}$.

Using the kernel function $\Phi: \Re^n \to F, x \mapsto \Phi(x)$, the sample set X' is mapped to the feature space F to obtain the mapped sample set $X'^{\Phi} = \{\phi(z_1), \phi(z_2), \cdots, \phi(z_N)\}$.

Construct the interclass scatter matrix S_B^{Φ} and the intraclass scatter matrix S_W^{Φ} in the feature space from the mapped sample set X'^{Φ}:

$$S_B^{\phi} = \frac{1}{c}\sum_{i=1}^{c}\left(u_i^{\phi} - u^{\phi}\right)\left(u_i^{\phi} - u^{\phi}\right)^T \tag{7}$$

$$S_W^{\phi} = \frac{1}{N}\sum_{i=1}^{c}\sum_{j=1}^{n_i}\left(\phi(z_{ij}) - u_i^{\phi}\right)\left(\phi(z_{ij}) - u_i^{\phi}\right)^T \tag{8}$$

where, $\phi(z_{ij})$ is a mapping sample in sample set X'^{Φ}, u_i^{ϕ} is the mean of the i-th class of mapping samples in X'^{Φ}, and $u^{\Phi} = \frac{1}{N}\sum_{i=1}^{N}\phi(z_i)$ is the total mean of all mapping samples in X'^{Φ}.

Then, the solution W_{DCT}^{ϕ} of the nonlinear DCT discrimination vector in the feature space is to maximize the following criterion:

$$J(W_{DCT}^{\phi}) = \frac{W_{DCT}^{\phi T} S_B^{\phi} W_{DCT}^{\phi}}{W_{DCT}^{\phi T} S_W^{\phi} W_{DCT}^{\phi}} \tag{9}$$

After derivation, it is easy to obtain that the optimal solution of W_{DCT}^{ϕ} is the eigenvector corresponding to the largest eigenvalues of the matrix $(S_W^{\phi})^{-1} S_B^{\phi}$.

4. ALGORITHM SUMMARY

In summary, the entire algorithmic flow of the DCT-based kernel forensic analysis method can be summarized as follows:

<u>Step 1</u>: Do the 2D DCT transform on each image in the original sample set X, select the appropriate DCT band for the transformed image according to the nonlinear discriminative ability value of the band, and do the column-wise quantization on the selected band. So far, a new one-dimensional training sample set X' is obtained.

<u>Step 2</u>: Map the sample set X' to the feature space F to get the mapped sample set X'^{φ} and construct the interclass scatter matrix and intraclass scatter matrix in the kernel space. Solve the optimal projection transformation matrix W_{DCT}^{ϕ} in the kernel space using Eq. (9). Here, the kernel function that implements the nonlinear mapping is the Gaussian kernel function, $k(z_1, z_2) = exp\left(\frac{-\|z_1 - z_2\|^2}{2\delta^2}\right)$, where δ^2 is set to be the variance of the training sample set X'. The nonlinear discriminative features of each sample $\phi(z)$ in X' are extracted:

$$\hat{y} = {W_{DCT}^{\phi}}^{T} \phi(\mathrm{z}) \tag{10}$$

Normalize $\hat{y}$ to $y = \frac{\hat{y}}{\|\hat{y}\|}$, where $\| \quad \|$ denotes the two-paradigm operation on vectors. Using this approach, a new sample set Y corresponding to X' can be obtained.

<u>Step 3</u>: Classify Y using the nearest neighbor classifier with cosine angle measure. For a given two arbitrary samples y_1 and y_2 the distance between them is defined as:

$$d(y_1, y_2) = -\frac{y_1^T \; y_2}{\|y_1\| \; \|y_2\|} \tag{11}$$

Figure 3 shows a schematic diagram of the entire identification process of the DCT-based KDA method.

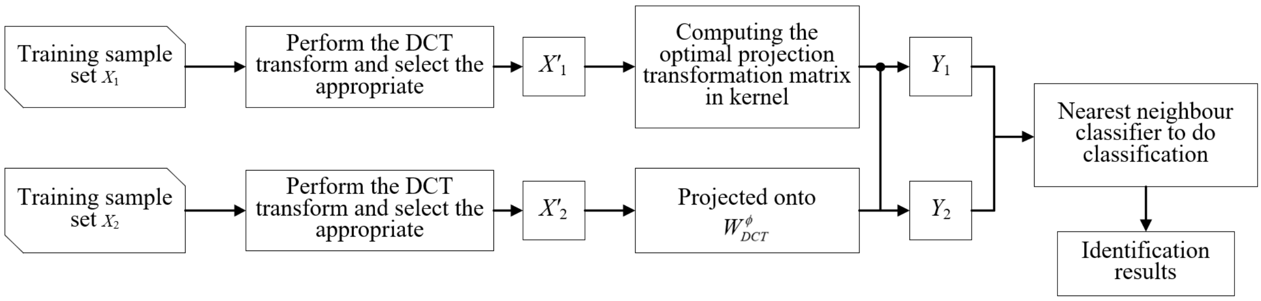

Figure 3. Identification steps of DCT-based KDA

5. EXPERIMENTAL RESULTS AND ANALYSIS

5.1 Introduction to the database

In this paper, two public image databases are used in the experiments, which are the FERET face database and AR face database.

(1) FERET face database

The FERET face database used in the experiments of this paper contains 200 people, 11 images per person totaling 2200 greyscale images. The size of each original greyscale image is 384×256. Since many images in the face database contain background and upper body parts, cropping is done on each image in the experiment to get an image of size 300×256. After that, the obtained images were subjected to the extraction process, and finally images of size 60*50 were obtained.

Figure 4. All images of a person in the FERET face library

Figure 4 shows all the images of a person in the FERET face library. The following are the detailed descriptions of these images: (a) frontal standard pose; (b) left tilt 15 degrees; (c) right tilt 15 degrees; (d) left tilt 40 degrees; (e) right tilt 40 degrees; (f) left tilt 25 degrees; (g) right tilt 25 degrees; (h) expression change; (i) illumination change; (j) left tilt 60 degrees; (k) right tilt 60 degrees.

(2) AR face database

The AR face database used in the experiments of this paper contains 26 images for each of 119 individuals. The size of each original image is 768×576, which is compressed to the size of 60×60.

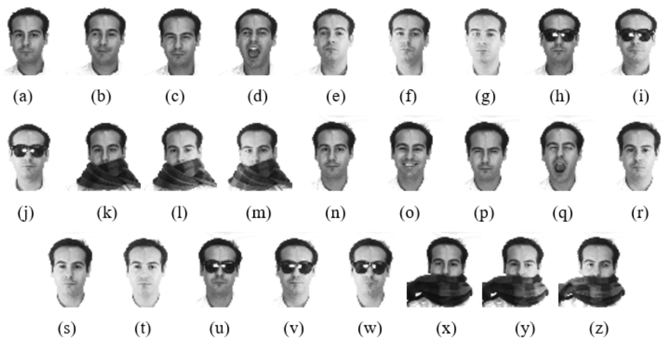

Figure 5. All images of a person in the AR face database

Figure 5 shows all the images of a person, where images numbered (a)-(m) are captured for the first time and images numbered (n)-(z) are captured for the second time. These images are capable of reflecting changes in various factors such as posture, expression, light, position, time, and the like. The following are detailed descriptions of these images: (a) and (n) normal expression; (b) and (o) smiling; (c) and (p) angry; (d) and (q) screaming; (e) and (r) left side illumination; (f) and (s) right side illumination; (g) and (t) omni-directional illumination; (h) and (u) spectacle occlusion; (i) and (v) spectacle occlusion and left side illumination; (j) and (w) spectacle blocking and right side light; (k) and (x) scarf blocking; (l) and (y) scarf blocking and left side light; (m) and (z) scarf blocking and right side light.

5.2 Experimental results and analyses of the DCT-based nuclear forensic analysis method

This subsection compares the DCT-KDA method proposed in this paper with KDA, DCT-LDA, and other methods on FERET and AR face databases.

5.2.1 Experimental results on the FERET database

The first two to six images of each person in the FERET database were sequentially selected as training samples in the experiment, and the rest were used as test samples.

Figure 6 shows the recognition rates for different numbers of DCT bands at three training samples. It is easy to see from Figure 6 that the best recognition results are achieved by selecting the lower frequency bands sequentially. In particular, the highest recognition rate of 74.63% is achieved when frequency bands 1 to 16 are selected. Figure 7 shows the original image and the image after DCT filtering: (a) the original greyscale image; (b) the image reconstructed from 1-16 bands after DCT filtering.

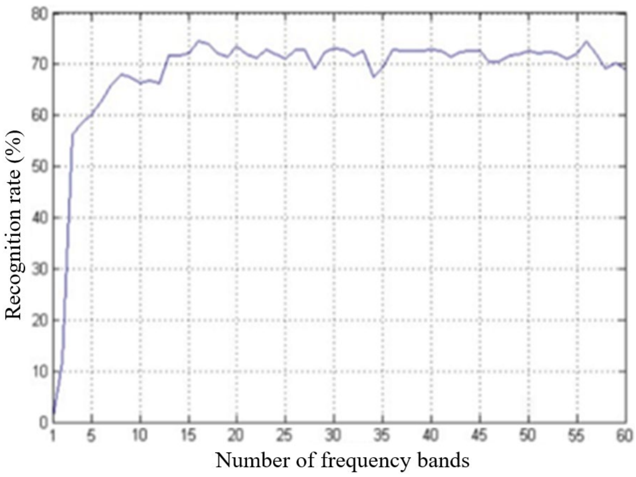

Figure 6. Recognition effect for different number of DCT bands

(a) (b)

Figure 7. Original image and reconstructed image after DCT filtering

In the experiments, the DCT-KDA method proposed in this paper is compared with the DCT-LDA method and the Nonlinear Discriminative Analysis (KDA) method. In the experiments, both the DCT-LDA and the methods in this paper use the same band selection criteria, and all methods use the same classifier, the nearest neighbor classifier. The recognition rates of the various methods are shown in Figure 8, which shows that the average recognition rates of DCT-KDA, KDA, and DCT-LDA are 80.42%, 78.18%, and 78.67%, respectively. Compared with the other two methods, the average recognition rate of this paper's method is at least 1.75% higher than the other methods. In addition, the method in this paper will save 41.66% (=(172.36-100.56)/172.36*100%) of the average computation time compared to the traditional nonlinear identification method KDA.

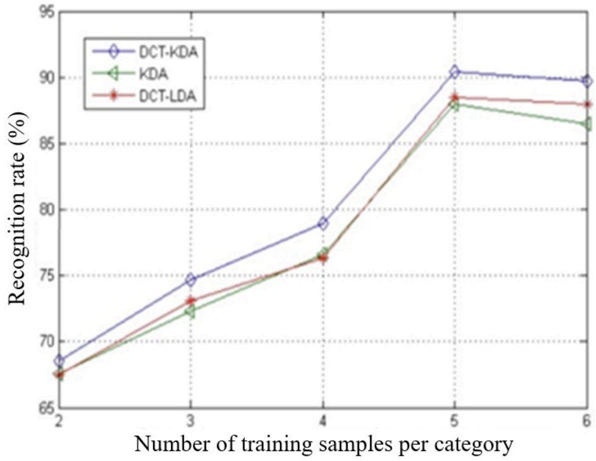

Figure 8. Comparison of recognition rates of various methods

5.2.2 Experimental results on the AR database

Two to eight images of each person in the AR database were sequentially selected as training samples and the rest as test samples in the experiment. Figure 9 shows the recognition rate for different numbers of DCT bands at four training samples. It can be seen that the highest recognition rate of 74.87% is achieved when bands 1 to 18 are selected. Comparison of recognition rates of various methods is shown in Figure 10, where it can be seen that the average recognition rates of DCT-KDA, KDA, and DCT-LDA are 80.09%, 75.99%, and 79.08%, respectively. Compared to the other two methods, the average recognition rate of this paper's method is at least 1.01% higher than the other methods. In addition, the method in this paper will save 53.86% (=(243.52-112.36)/243.52*100%) of the average computation time compared to KDA.

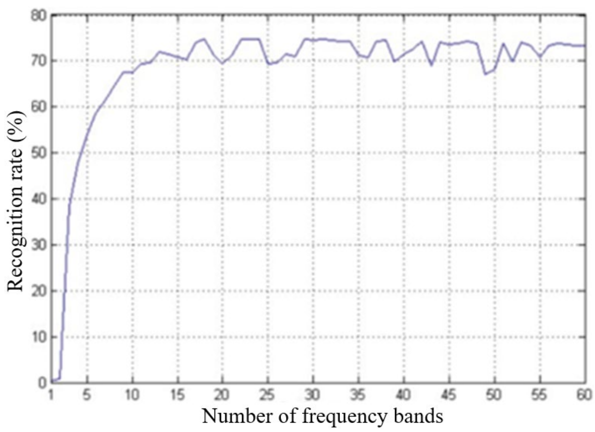

Figure 9. Recognition effect for different number of DCT bands

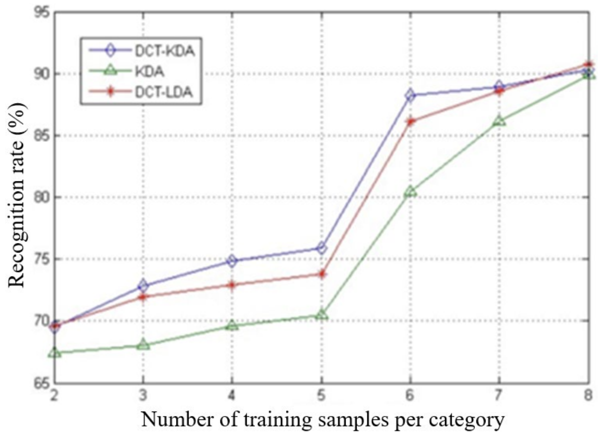

Figure 10. Comparison of recognition rates of various methods

Experiments on both the FERET library and the AR library imply that the method in this paper can complete the extraction of nonlinear discriminative features very quickly and is a fast and effective nonlinear method.

6. CONCLUSION

In this study, the traditional DCT-based discriminative analysis approach was examined, and its scope was extended from linear to nonlinear methods through the design of the DCT-KDA algorithm. The DCT was applied to facial images, and appropriate frequency bands were selected to retain relevant biometric features. Nonlinear discriminative features were then extracted from these frequency bands using KDA. The effectiveness of the proposed algorithm was evaluated through experiments conducted on the FERET and AR face databases. The results indicate that the DCT-KDA algorithm enhances recognition performance while also achieving faster recognition speeds, demonstrating its potential for practical application in biometric systems.

This work contributes to the field by addressing the limitations of traditional DCT-based linear methods, offering a more robust framework that integrates the advantages of frequency-domain transformations with nonlinear feature extraction. By focusing on the low-frequency components that encapsulate essential facial information, and discarding high-frequency elements prone to noise, the algorithm ensures efficient feature representation. The combination of DCT and KDA provides a scalable solution with strong discriminative capabilities, making it suitable for real-time recognition tasks. Further research could explore the application of this method to other biometric modalities and investigate its performance under varying environmental conditions, such as different lighting and occlusion levels.

This algorithm's ability to improve recognition accuracy and computational efficiency highlights its relevance for biometric authentication and verification in high-demand environments. The use of the FERET and AR face databases also ensures that the method is validated against well-established benchmarks, reinforcing the significance of these findings within the broader context of biometric research.

REFERENCES

[1] Fukunaga, K. (2013). Introduction to Statistical Pattern Recognition. Elsevier.

[2] Joliffe, I.T. (2002). Principal Component Analysis. Springer.

[3] Benouareth, A. (2021). An efficient face recognition approach combining likelihood-based sufficient dimension reduction and LDA. Multimedia Tools and Applications, 80(1): 1457-1486. https://doi.org/10.1007/S11042-020-09527-9

[4] Arisandi, D., Syahputra, M.F., Purnamawati, S., Hizriadi, A., Azra, M.H. (2021). Face recognition for a student violation point system in schools using the fisherface algorithm. In Journal of Physics: Conference Series, 1898(1): 012024. https://doi.org/10.1088/1742-6596/1898/1/012024

[5] Zhou, B., Liu, W., Zhang, W., Lu, Z., Tan, Q. (2022). Multi-kernel graph fusion for spectral clustering. Information Processing & Management, 59(5): 103003. https://doi.org/10.1016/j.ipm.2022.103003

[6] Mohammed, N.N. (2022). Improved regularized multi-class logistic regression for gene classification with optimal kernel PCA and HC algorithm. In Worldwide Congress on "Genetics, Geriatrics and Neurodegenerative Diseases Research", Zakinthos, Greece, pp. 273-279. https://doi.org/10.1007/978-3-031-31982-2_31

[7] Chen, W.S., Ge, X., Pan, B. (2022). A novel general kernel-based non-negative matrix factorisation approach for face recognition. Connection Science, 34(1): 785-810. https://doi.org/10.1080/09540091.2021.1988904

[8] Zhao, H., Yuen, P.C. (2008). Incremental linear discriminant analysis for face recognition. IEEE Transactions on Systems, Man, and Cybernetics, Part B (Cybernetics), 38(1): 210-221. https://doi.org/10.1109/TSMCB.2007.908870

[9] Lee, D., Krim, H. (2017). 3D face recognition in the Fourier domain using deformed circular curves. Multidimensional Systems and Signal Processing, 28: 105-127. https://doi.org/10.1007/s11045-015-0334-7

[10] Antonijevic, M., Strumberger, I., Lazarevic, S., Bacanin, N., Mladenovic, D., Jovanovic, D. (2022). Robust encrypted face recognition robot based on bit slicing and Fourier transform for cloud environments. Journal of Electronic Imaging, 31(6): 061808. https://doi.org/10.1117/1.JEI.31.6.061808

[11] Hasimah, A., Ho, Y.K., Khairunizam, W.A.W., Mohamed, E., Norrima, M. (2022). Classification of body mass index based face images using facial landmarks approach and PCA plus LDA. In Proceedings of International Conference on Artificial Life and Robotics, pp. 1020-1024. https://doi.org/10.5954/ICAROB.2022.OS32-9

[12] Saritas, O.F., Ozturk, S. (2023). A blind CT and DCT based robust color image watermarking method. Multimedia Tools and Applications, 82(10): 15475-15491. https://doi.org/10.1007/S11042-022-13928-3

[13] Vishwakarma, V.P., Dalal, S. (2020). Generalized DCT and DWT hybridization based robust feature extraction for face recognition. Journal of Information and Optimization Sciences, 41(1): 61-72. https://doi.org/10.1080/02522667.2020.1721593

[14] Ernawan, F., Ariatmanto, D. (2023). An efficient adaptive scaling factor for 4×4 DCT image watermarking. Multimedia Tools and Applications, 82(6): 8603-8621. https://doi.org/10.1007/S11042-022-

14220-0
[15] Varyani, M., Narware, P., Banafar, L.S. (2019). PCA and DCT Based Approach for Face Recognition. Journal of Trend in Scientific Research and Developmental, 3(3): 1286-1290. https://doi.org/10.31142/ijtsrd23283
[16] Chen, S., Zhao, C., An, S. (2019). Study on processing of infrared thermogram of ankle soft tissue injury with LDA based on DCT transform. Optics in Health Care and Biomedical Optics IX, 11190: 267-274. https://doi.org/10.1117/12.2537506
[17] Benziane, A., Awang, S., Lebcir, M. (2021). Development and implementation of a video watermarking method based on DCT transform. The International Arab Journal of Information Technology, 18(2): 140-147. https://doi.org/10.34028/IAJIT/18/2/2
[18] Gomez-Coronel, S.L., Moya-Albor, E., Brieva, J., Romero-Arellano, A. (2023). A robust and secure watermarking approach based on Hermite transform and SVD-DCT. Applied Sciences, 13(14): 8430. https://doi.org/10.3390/APP13148430
[19] Zhang, J., Zhou, S. (2024). Structured orthogonal random features based on DCT for kernel approximation. Neurocomputing, 610: 128640. https://doi.org/10.1016/j.neucom.2024.128640